AN IDENTIFICATION SCHEMA FOR A GENERALIZED PREISACH MODEL

A. Ktena, D.I. Fotiadis, C.V. Massalas and P.D. Spanos

6 – 2001

Preprint, no 6 – 01 / 2001

Department of Computer Science
University of Ioannina
45110 Ioannina, Greece

An Identification Schema for a Generalized Preisach Model

A. Ktena[(1)], D. I. Fotiadis[(1)], C. V. Massalas[(2)] and P. D. Spanos[(3)]

(1) Dept. of Computer Science, University of Ioannina, GR 45110 Ioannina, Greece
(2) Dept. of Materials Science, University of Ioannina, GR 45110 Ioannina, Greece
(3) Dept. of Mechanical Engineering and Materials Science,
George R. Brown School of Engineering, Rice University, Houston, USA

ABSTRACT

A generalized modular Preisach model able to adjust to different systems with hysteresis is presented. The identification schema accompanying it is using data from a major hysteresis curve and a least-squares fitting procedure for the parameters of the characteristic density. In a hysteresis model following the Preisach formalism, the output sequence, $\mathbf{f}(t)$, is obtained by integrating the characteristic probability density function, $\rho(\alpha,\beta)$, of the elementary hysteresis operators, γ_{ab}, operating on the input sequence $\mathbf{u}(t)$ over the Preisach plane. The operator can be chosen from a selection of scalar or vector ones. Once the operator is chosen and the Preisach plane adjusted accordingly, the parameters of characteristic density are determined through a least-squares procedure minimizing the error between the experimental major curve and the calculated one. Results using two different operators and a comparison with experimental hysteresis data on two different magnetic samples and a shape memory alloy sample, involving both major and minor curves, are presented.

Keywords: Preisach modeling; Hysteresis.

1. INTRODUCTION

Hysteresis is a phenomenon encountered in several natural, mechanical, engineering, and socioeconomical systems. The causes differ from system to system: they depend on the components and structure of the system and the laws governing their behavior and interaction. The effect however is common in all of them: the output is *delayed* with respect to the input. This common phenomenological behavior of hysteretical systems has been the motivation behind this work that aims to developing a general model of hysteresis capable to adjust and be identified for various systems.

The vehicle for this is the Preisach formalism [1], a scalar model of ferromagnetic hysteresis (magnetization vs. field) that, lately, has been extended to applications in other systems with hysteresis like shape memory alloys (strain vs. temperature) [2], in the elastic behavior of rocks (strain vs. stress) [3], in economics (output vs. expansionary or contractionary input shocks) [4]. The traditional scalar model can also be extended to a vector formulation [5-7] appropriate for vector hysteresis processes. The model, in its scalar and vector formulation, has found applications in magnetic recording material modeling [8], in the calculation of losses in electrical steel laminations [9], in the control of shape memory alloys (SMA) actuators [10] and as core model in finite element calculations [11]. The identification of Preisach models is carried out either through detailed measurements of the characteristic density [3, 10, 12, 18] or through determining the parameters of the density based on a major loop measurement [8, 5-7, 22].

The Preisach formalism presents the advantage of being abstract enough to adjust itself to various systems through the appropriate selection of hysteresis operator and chartacteristic density. The phenomenon of hysteresis and the type of hysteresis modeled by the proposed method is discussed in section 2. Section 3 deals with the modeling of the process of hysteresis and the building blocks of the model: a selection of hysteresis operators and their features, the classical formalism, the vector formulation and the identification process. A systematic approach to an identification method using the major loop characteristic and a least squares algorithm that optimizes the density parameters is described. In order to test the new identification method and demonstrate the general and modular nature of the model, results using two different operators are presented in section 4. The results are compared with experimental data for magnetic and SMA samples.

2. HYSTERESIS

Not any delay can be referred to as hysteresis. Visintin [13] defines hysteresis as the *rate independent memory effect*. According to this definition, in a system with hysteresis the current output is a function of the current input as well as previous inputs and/or the initial state. In other words, the system can store information, it has *memory*. For every input there may be more than one equilibrium states. The resulting state depends on the history of the system, on the previous equilibrium states. When a system with hysteresis is *bistable* is characterized by a hysteresis loop like the one shown in Fig. 1. The curve is traced along the path ABC (descending branch) or CDA (ascending branch). For $u \geq u_{s+}$ (or $u \leq u_{s-}$), the output is increasing (or decreasing) monotonically with the input,

hysteresis vanishes, the processes are reversible and the resulting states are uniquely defined and *stable*. For $u_{s-} < u(t) < u_{s+}$, $f(t)$ is a *metastable* state and a nonlinear function of previous states [13]. If the loop ABCDA delimits the space of all possible states for any given input, it is called a *major loop*. As it will be discussed later, a major loop measurement provides a lot of information about the system. The loop in Fig. 1 is symmetric around the origin, typical of ferromagnets but not necessarily of other systems. A point inside the major loop can be attained through several trajectories called *minor loops*.

The definition of hysteresis adopted in this work refers to it as rate independent. This suggests a quasistatic treatment of the problem since, in actual systems, the rate of change of the input does have an effect on the output. The assumption here is that the rate of change is slow enough to allow for any transients to die out. The model can be applied to such systems only.

3. MODELING OF HYSTERESIS

In ferromagnets, hysteresis occurs during the switch from positive to negative magnetization. According to the Weiss theory, the material is made of a large number of elementary magnets (domains). Under an applied magnetic field $H(t)$, the state of each elementary magnet depends on the external field as well as an internal interaction field with the other domains which is a function of the magnetization state, $M(t)$. Hence the resulting magnetization state contains a positive feedback mechanism leading to hysteresis: $M(t) = M(H(t), M(t))$.

Modeling of magnetic hysteresis falls under two broad categories: micromagnetic and macroscopic modeling. The macroscopic approach features hysteresis operators and Preisach-type modeling and is discussed in the following section. The micromagnetic approach is based on the minimization of the free energy equation for a collection of elementary magnets (domains, particles) [14,15]. The energy equation contains terms such as the exchange energy $A \cdot [\nabla \cdot \mathbf{M}]^2$, the applied field energy $\mathbf{M} \cdot \mathbf{H}_{app}$, the anisotropy energy $K_1 \cdot (\mathbf{n} \cdot \mathbf{M})^2 + K_2 \cdot (\mathbf{n} \cdot \mathbf{M})^4 + \cdots$, the self magnetostatic energy $\frac{1}{2}\mathbf{M} \cdot \mathbf{H}_{int}(\mathbf{M})$, etc., where A is the exchange constant referring to short range (spin-spin) interactions, $\mathbf{H}_{app}$ is the externally applied field, $K_1, K_2, \ldots$ are the anisotropy constants, $\mathbf{n}$ is a unit vector, and $\mathbf{H}_{int}$ is the field corresponding to long range magnetostatic interactions and a function of the magnetization as described above. This approach allows for a detailed description of the microstructure and takes into account the underlying physics. But, in order to model the behavior of a physical system a large number of interacting particles is needed and this leads to cumbersome and long calculations which prohibit the use of this model in simulations or control applications.

SMAs, on the other hand, undergo a phase transformation with temperature. At low temperatures, the martensitic and austenitic phases coexist and behave plastically while at

higher temperatures the martensitic phase vanishes and the material behaves elastically recovering its former shape. Hysteresis is evident in the transformation from the austenitic to the martensitic phase (forward) and vice versa (reverse) and it is due to the friction caused by the movement of the phase interfaces. Because of irreversible changes (plastic deformations) in the microstructure, the two transformations are not identical to each other. The phenomenology of this is evident in the asymmetrical and skewed hysteresis loops (figs. 7-8). The cause of hysteresis in SMAs lies in [2].

Like in ferromagnets, the modeling approaches fall under two categories. One category includes macroscopic models based on hysteresis operators with Preisach being the most popular. The other approach is based on thermomechanics and the minimization of the free energy equation. The latter can be a function of stress, temperature, the martensitic volume fraction, thermal, plastic and trasnformation strains and back and drag strain. This method offers the obvious advantage of internal state variables but poor results are obtained when compared to experimental data. [2].

3.1 Hysteresis operators

A key feature in the class of macroscopic models, where the Preisach formalism belongs, is the *hysteresis operator*, i.e. an operator that posseses the memory property and the rate independence property. The play, stop, Preisach and KP operators are shown in Fig. 2. The first two operators are common mainly in elastoplasticity (see Ref. 16 for a more extensive discussion).

The classical Preisach operator (Fig. 2c) is:

$$\gamma_{ab} = \begin{cases} +1, & u > a \\ -1, & u < b \end{cases}.$$

The shape of the operator is that of an elementary hysteresis loop with discontinuous transitions at points a and b. The KP operator (Fig. 2d), named after Krasnoselskii-Pokrovskii [17] who, among others, investigated the mathematical properties of hysteresis operators describes a smooth transition between the two states:

$$\gamma_{ab} = \begin{cases} 1 & u > b + x \\ -1 + 2\frac{u}{x}(u - b) & b < u < b + x \\ -1 & u < b \end{cases}, \text{ for the descending curve}$$

$$\gamma_{ab} = \begin{cases} -1 & u < a - x \\ 1 - 2\frac{u}{x}(u - a) & a - x < u < a \\ 1 & u > a \end{cases}, \text{ for the ascending curve}$$

where x is the rise (or fall) distance.

The last operator (Fig. 2e) is a modification of the classical Preisach operator appropriate for the modeling of mechanical hysteresis (stress/strain, SMAs) [2]. The hysteresis curves observed in SMAs (Figs. 7-8) are traced in the opposite direction than the magnetic ones and the output variable varies from 0 to 1:

$$\gamma_{ab} = \begin{cases} 0, & u > a \\ +1, & u < b \end{cases}$$

3.2 The Preisach formalism

According to the Preisach formalism, hysteresis is the result of superposition of scalar local hysteresis operators γ_{ab} (Fig. 2c). The system being modeled is viewed as a collection of subcomponents each of which has a hysteresis characteristic γ_{ab} with different switching points (a,b). The displacement of the loop from the origin, $u_d = \frac{a+b}{2}$, corresponds to the effective interactions experienced by a given component. If the subcomponents are isolated or the sum of interactions one of them experiences is zero the corresponding loop is centered at the origin and $a = -b$. The loop halfwidth, or half distance between the two critical values is $u_c = \frac{a-b}{2}$. When $a = b$ a degenerate loop of zero halfwidth, $u_c = 0$, is obtained.

The system is modeled as a distribution of upper and lower switching points (a,b) obtained from the characteristic density of the system $\rho(a,b)$ defined over the Preisach plane (Fig. 2a) [18]. The plane is bounded by $u_c = 0$ (otherwise the lower switching point b is greater than the upper switching field a which violates the second law of thermodynamics), $u = u_{s+}$ and $u = u_{s-}$ where u_{s+} and u_{s-} are the input values leading to positive and negative saturation respectively: $\forall a,b \quad a \le u_{s+}, b \ge u_{s-}$.

The response of the system, $f(t)$, to an input, $u(t)$, is the integral of the output states of each elementary loop weighed by the probability density function $\rho(a,b)$:

$$f(t) = \iint_{a \ge b} \rho(a,b)\gamma_{ab}u(t)dadb$$

Because of the integration of a probability density function, the formalism allows for continuous hysteresis to be described even though a discontinuous hysteresis operator is used. Since the model is quasistatic, time is discretized and an input sequence $u_0, u_1, ..., u_n$ is assumed instead of a continuous input time function. When an input $u_0 < u_{s-}$ is applied, the system "saturates" in the negative state where all the operators are in the -1-state. Increasing the input to $u_1 > u_{s-}$ all operators with $u_{s-} < a < u_1$ will switch to $+1$. A horizontal boundary separating the regions of $+1$- and -1- states is established at $a < u_1$ and the change in output, $\Delta f = f_1 - f_0$, is obtained by integrating the density over the triangle ABC. Decreasing the input to $u_{s-} < u_2 < u_1$, all operators with

$b > u_2$ will revert to -1 and a perpendicular boundary segment appears (Fig. 3a). The change in output is then given by the integral over the triangle CDE. This way, at the end of an input sequence a *staircase boundary* is established between areas of positive and negative state. The horizontal and vertical segments, a direct consequence of the discontinuity of the operator at the switching points, clearly indicate the past input extrema. Therefore, the boundary serves as *memory* keeping track of the history of the system. The integrals of the density over the triangular area of change are called *Everett functions* [12] and can be used for the identification and the *inverse* model [20].

Mayergoyz has proven that in order for a system to be modeled according to the Preisach formalism the necessary and sufficient condition is that it posseses the wipe-out and congruency properties [18]. This is a limitation towards the waiving of which a lot of effort has been invested because real systems do not comply with the requirement. Another bothersome characteristic of the traditional Preisach model is the ability to model irreversible changes only. This is a direct consequence of the hysteresis operator acting as a switch.

3.3 The vector formulation

The model described so far is an inherently scalar model useful for applications where the 1D treatment is adequate. A vector model following the Preisach formalism can be obtained by substituting the scalar operator by a vector (2D) one. Two vector operators are shown in Fig. 4. The SW astroid [19] (Fig. 4a) is widely used in micromagnetic modeling. It is the locus of the equation $u_e^{2/3} + u_h^{2/3} = 1$, where u_e and u_h are the components of the input u(t) along the easy and hard axis respectively. The solution is the tangent to the astroid passing from the tip of the input vector. Switching occurs when the output vector crosses the astroid from the inside out. Otherwise the output vector rotates reversibly. Note that the astroid equation results from the minimization of the free (Gibbs) energy equation for an ellipsoidal magnetic particle with uniaxial anisotropy under the influence of an applied field. It is not an abstract mathematical structure like its scalar counterpart.

The second vector operator (Fig. 4b) is the first order approximation of the SW astroid: $u_e + u_h = 1$ and is computationally more efficient but without physical attributes.
The vector formulation is:

$$\boldsymbol{f}(t) = \iint_{a \geq b} \rho(a,b)\boldsymbol{\gamma}_{ab}\boldsymbol{u}(t)\,da\,db\,.$$

For a given time t and a point (a,b) on the Preisach plane, the vector hysteresis operator $\boldsymbol{\gamma}_{ab}$ acts on the vector input $\boldsymbol{u}(t)$. The result is weighed by the probabilty density function $\rho(a,b)$ and the output $\boldsymbol{f}(t)$ is obtained by integrating over the Preisach plane. The vector properties of this model are very good and in agreement with experiments [5-8]. The vector formulation does not possess the congruency property since it allows for reversible processes (rotation of the output vector without switching from + to -). The

lack of the congruency property makes it appropriate for modeling systems that do not have this property but it is not a Preisach model anymore in the classical sense [18].

Replacing the classical operator by a vector one has an important effect on the shape of the boundary. It no longer consists of horizontal and vertical segments neatly indicating past input extrema. This is expected since the vector operator is not discontinuous at points a and b. Note that the same effect is observed when the scalar hysteresis operator of Fig. 2a is used. Therefore, identification and inversion techniques used with the traditional operator can no longer apply.

The above formulation assumes a perfectly oriented system, i.e. all the elementary subcomponents are oriented in the same direction. Where needed, *dispersion* of orientations can be added by superimposing the responses of angularly distributed perfectly oriented models:

$$\boldsymbol{f}(t) = \int_{-\pi/2}^{\pi/2} \rho(\phi)d\phi \iint_{a\geq b} \rho(a,b)\boldsymbol{\gamma}_{ab}\boldsymbol{u}(t)dadb\,.$$

where $\rho(\varphi)$ is a probability density function of angles.

Another vector formulation using a vector "play" operator (Fig. 2a) and its relationship to the classical model is described in [21]. It has interesting vector properties and it regresses to the scalar Preisach model for a specific choice of parameters, but only irreversible processes are predicted. The reversible component has to be added on.

3.4 Identification

The identification of Preisach-type modeling consists of determining the characteristic density $\rho(a,b)$. In the case of the classical model where the Everett functions are defined, the distribution can be measured in detail. The density can then be constructed from the measurements. This has produced good results in applications [3, 5,10] where the density is measurable and the assumptions of the traditional scalar model can apply.

The alternative approach, which is the one discussed in this work, is to fit the parameters of a known density to some points on a major hysteresis curve. This method is more appropriate for use with a general application model because it is not restricted by the type of material or system, the 1D or 2D treatment of the problem and the ability to measure the Everett functions. The only measurement needed is that of a major hysteresis curve. The issues that need to be addressed when using this method are the choice of the probability density function and the parameter fitting procedure.

The bivariate probability density function of upper and lower switching points can be equivalently expressed in terms of the transformation $u'_c = \frac{a-b}{\sqrt{2}}$ and $u'_d = \frac{a+b}{\sqrt{2}} : \rho(a,b) = \rho(u'_c, u'_d)$ (Fig. 3).

There are systems that can support the assumption that the variables u'_c and u'_d are independent and therefore $\rho(a,b)=\rho(u'_c,u'_d)=\rho(u'_c)\rho(u'_d)$. The density can then be constructed as the product of two single-variable different densities instead of one bivariate density [5-7, 11]. The expectations (mean values), μ_c, μ_d and μ_a,μ_b, and the variances, σ_c^2, σ_d^2, and σ_a^2, σ_b^2, of the probability density function of the four variables are related (for simplicity, we use $u'_c=c$ and $u'_d=d$):

Statement 1. If the random variables c and d are independent then

$$E[\rho(a,b)]=E[\rho(c,d)]=\mu_c\cdot\mu_d=\frac{1}{2}\left(\mu_a^2-\mu_b^2\right)$$

Proof
It is known that

$$E[\rho(a,b)]=E[\rho(c,d)]=E[\rho(c)]\cdot E[\rho(d)]=\mu_c\cdot\mu_d$$

but

$$\mu_c=E(c)=E\left(\frac{a-b}{\sqrt{2}}\right)=\frac{1}{\sqrt{2}}(\mu_a-\mu_b)$$

and

$$\mu_d=E(d)=E\left(\frac{a+b}{\sqrt{2}}\right)=\frac{1}{\sqrt{2}}(\mu_a+\mu_b)$$

therefore, $\mu_c\cdot\mu_d=\frac{1}{2}\left(\mu_a^2-\mu_b^2\right)$.

Statement 2. If the random variables c and d are independent then $\sigma_a^2=\sigma_b^2=2\cdot\left(\sigma_c^2+\sigma_d^2\right)$.
Proof
Since c and d are independent $Cov(c,d)=E[c\cdot d]-E[c]\cdot E[d]=0$.
but

$$E[c\cdot d]=E\left[\frac{(a-b)\cdot(a+b)}{2}\right]=E\left[\frac{a^2-b^2}{2}\right]=\frac{1}{2}\left(E[a^2]-E[b^2]\right),$$

and

$$E[c]\cdot E[d]=\mu_c\cdot\mu_d=\frac{1}{2}\left(\mu_a^2-\mu_b^2\right)$$ (from statement 1),

therefore,

$$E[a^2]-E[b^2]=\mu_a^2-\mu_b^2\Leftrightarrow E[a^2]-\mu_a^2=E[b^2]-\mu_b^2\Leftrightarrow\sigma_a^2=\sigma_b^2$$

Using the inverse variable transformation $a = \sqrt{2}(c + d)$ and $b = \sqrt{2}(d - c)$, $\sigma_a^2 = E[a^2] - (E[a])^2$.
but

$$E[a^2] = E\left[\left(\sqrt{2}(c + d)\right)^2\right] = 2(E[c^2] + E[d^2] + 2 \cdot E(c \cdot d)),$$

and

$$(E[a])^2 = \left(E\left[\sqrt{2}(c + d)\right]\right)^2 = 2(E[c] + E[d])^2 = 2(\mu_c^2 + \mu_d^2 + 2 \cdot E(c \cdot d)),$$

therefore,

$$\sigma_a^2 = 2(E[c^2] + E[d^2] - \mu_c^2 - \mu_d^2) = 2(\sigma_c^2 + \sigma_d^2).$$

Lets take a look into the physical meaning of the above statements. The assumption that the u_c' and u_d' are independent variables is valid in the hysteresis modeling of ferromagnets, for example. In the case of ferromagnets, the hysteresis loops are symmetrical and centered at the origin: $f(u(t))|_{\dot{u}<0} = -f(-u(t))|_{\dot{u}>0}$, e.g. the coercive field (the input value at which the output is zero) is of the same magnitude in both the ascending and descending branch but of opposite sign (Figs. 5-6). From a modeling point of view, this is a consequence of statement 2. In order to obtain symmetrical hysteresis loops like the ones in Figs. 5-6, $\sigma_a^2 = \sigma_b^2$ must hold. In magnets, the transformation variables u_c' and u_d' correspond to the coercivity and interaction fields of an elementary hysteresis loop (operator). The elementary loop can be considered to represent the hysteresis characteristic of a magnetic domain or particle in the material with coercivity u_c' and under the influence of an interaction field u_d'. The coercivity of a particle or domain is a function of temperature, size and shape. The interaction field, on the other hand, is an effective field acting on the particle or domain and containing contributions of short range (spin-spin) and long range (dipole-dipole) interactions. There is no reason to assume there is a correlation between the two quantities.

Statement 1 implies that the expected value of the Preisach density is zero for $\mu_a = \mu_b$. This is the case for loops centered at the origin, like the ones observed in ferromagnets. Then, at least one of the two terms of the product $\mu_c \cdot \mu_d$ must be zero. The expected value of coercivities, μ_c, cannot be zero because in that case half of the density would lie outside the Preisach plane, where $b > a$. But, the assumption that the mean value of interactions is zero is valid from a physics point of view.

4 RESULTS AND DISCUSSION

The most commonly used pdf in Preisach modeling is the normal one [6, 7, 22] but lorentzians [5, 11] or the arctan function [21] has been used as well. In [6] the Preisach density is built as a product of a gaussian (for the coercivities) and a lorentzian (for the interactions). In the remaining of this work we will concentrate on single-variable and bivariate normal distributions.

In [6, 7] a vector Preisach model was identified for two samples of ferromagnets: the homogeneous $Sm_2Fe_{14}Ga_3C_2$ (single phase) and the inhomogeneous $Sm_2Fe_{14}Ga_3C_2$/α-Fe (two-phase). The experimental data was found in the literature [23]. The microstructure of the two magnets is quite different, with exchange coupling between the hard ($Sm_2Fe_{14}Ga_3C_2$) and the soft (α-Fe) phase playing an important role in the second one. The identification procedure used in [6, 7] is outlined next. It will be referred to as "old" in order to distinguish it from the one that will be introduced afterwards and will be referred to as "new". The results labeled "old" in Figs. 5-6 were obtained using the vector model with dispersion and the "old" identification method. The Preisach density is built as a product of two gaussians, $\rho(u_c)$ and $\rho(u_d)$, of the form:

$$\rho(u_c) = \frac{1}{\sqrt{2\pi\sigma_c^2}} \exp\left[-\frac{(u_c-\mu_c)^2}{2\sigma_c^2}\right] \text{ and } \rho(u_d) = \frac{1}{\sqrt{2\pi\sigma_d^2}} \exp\left[-\frac{(u_d-\mu_d)^2}{2\sigma_d^2}\right].$$

The role of each one of the four parameters μ_c, σ_c, μ_d, σ_d on the shape of the hysteresis curve is different and related to physical parameters:

- μ_c controls the coercivity of the loop, i.e. the point at which the curve intersects the input (field) axis. Because the vector model with dispersion is used, the empirical rule for finding the value of μ_c is $H_c = 3\mu_c$ where H_c is the measured coercivity of the loop.
- μ_d is fixed to 0 as explained above.
- σ_c and σ_d affect the shape of the loop and are related to the S* loop parameter. S* is the slope of the loop around the coercivity, $S^* = \frac{dM}{dH}|_{H_c}$. In ferromagnets, S* is related to interactions, *i.e.* a higher S* suggests strong exchange interactions. Interestingly enough, from a modeling point of view, it is σ_d that primarily affects S*. Finding appropriate values for σ_c and σ_d is the most difficult part in this process being more of an art rather than a science.

It has already been mentioned that in Figs. 5-6, the simulated loops labeled "old model" were obtained using a vector model with dispersion. Therefore, a pdf of angles is also involved; it is a gaussian centered at 0^o with its standard deviation being the sole parameter controlling the squareness S of the loop, and therefore easy to determine. S is the ratio of the output at zero input over the maximum output value; in the case of

ferromagnets this corresponds to the ratio of remanent to saturation magnetization: $S = \frac{f|_{u=0}}{f_{max}} = \frac{M_r}{M_{sat}}$.

The "old" method uses a Preisach density built as product of two densities and four parameters (S, S*, H_c and M_s) of the major loop. It is a simple method but not systematic. It yields good results but the symmetry of the magnetic hysteresis loops has been a strong ally. Can it be used to systems without symmetric loops, e.g. SMA loops? The answer is negative.

The need to come up with a more systematic identification method applicable to as many classes of systems as possible pointed to the direction of using a bivariate probabilty density function as a basis for the Preisach distribution and apply a least-squares curve - fitting procedure.
The obvious bivariate pdf to start with is the normal one. The Preisach density is of the form:

$$\rho(a,b) = \frac{1}{2\pi\sigma_a\sigma_b\sqrt{1-r^2}} \exp\left[-\frac{1}{2(1-r^2)}\left(\left(\frac{a-\mu_a}{\sigma_a}\right)^2 - 2r\left(\frac{a-\mu_a}{\sigma_a}\right)\left(\frac{b-\mu_b}{\sigma_b}\right) + \left(\frac{b-\mu_b}{\sigma_b}\right)^2\right)\right]$$

There are five parameters to be determined: $\mu_a, \mu_b, \sigma_a, \sigma_b, r$ where r is the correlation parameter between a and b. For r=0, $\rho(a,b) = \rho(a)\rho(b)$.
The correlation parameter r has a slight effect on the shape of the loop; high positive values yield slightly higher squareness. So r is generally taken to be 0.

- When $\mu_a > \mu_b$ the hysteresis loop shifts to the left while when $\mu_a < \mu_b$ it shifts to the right.
- When $\sigma_a > \sigma_b$ the hysteresis loop is asymmetric and skewed with the bottom part wider (Fig. 7).
- When $\sigma_a < \sigma_b$ the hysteresis loop is again asymmetric and skewed with the upper part wider.

The values of the parameters are obtained through a least-squares curve-fitting procedure. Instead of using four parameters of the major loop and relate their values to the density parameters, an array of i points of the experimental loop is fed to the least squares algorithm along with an array of initial estimates of the parameters and the algorithm iterates on the parameter values until $\sum_i (f_{mod} - f_{exp})^2 < \varepsilon$, where ε is a small positive number. The value of ε used in the following results is 10^{-4}.

The results presented in the following sections have all been obtained with the scalar model adjusted appropriately for each material. The algorithms used follow:

- The algorithm for the model
  1. The KxK Preisach plane is initialized
  2. The input sequence u(t), t=1:T, is initialized

3. The Preisach plane pp(a,b) is defined
   3.1 if the classical operator is used then a > b
   3.2 else if the SMA operator is used then b < a
4. The Preisach density ρ(a,b) is constructed and distributed over the plane
5. For t=1:T
   5.1 call hysteresis operator (classical or SMA)
   5.2 pp(a,b)=γ(a,b)*u(t)
   5.3 f(t,a,b)=ρ(a,b)*pp(a,b)
   5.4 compute output $f(t) = \sum_a \sum_b f(t,a,b)$

- The algorithm for the classical Preisach hysteresis operator

1. if $u(t)-u(t-1)<0$ and $u(t)<b$ then $pp(a,b)=-1$
2. else if $u(t)-u(t-1)>0$ and $u(t)>a$ then $pp(a,b)=1$
3. else $pp(a,b)=pp(a,b)$

- The algorithm for the SMA hysteresis operator

1. if $u(t)-u(t-1)<0$ and $u(t)<b$ then $pp(a,b)=1$
2. else if $u(t)-u(t-1)>0$ and $u(t)>a$ then $pp(a,b)=0$
3. else $pp(a,b)=pp(a,b)$

Simulation of magnetic hysteresis

In the modeling of magnetic hysteresis, the input variable is the applied field and the output variable is the magnetization. The output is normalized with respect to the maximum value attained experimentally, or saturation magnetization, and ranges from -1 to +1. The scalar Preisach model used for ferromagnets is the classical one with the operator shown in Fig. 2c and the Preisach plane shown in Fig. 3a. The Preisach plane is coded as a $K \times K$ array. K depends on the desired degree of discretization and the maximum experimental input values observed. Each element of the array holds a hysteresis operator and the height (weight) of the density at the given point. The input is operated on by γ_{ab} at each element, its output state is decided and then multiplied by the weight. Summing over the weighed outputs of each element yields the aggregate output for a given input.

The initial parameter estimates fed to the least-squares algorithm are obtained as follows:

Since the loops are symmetrical, $\hat{\mu}_a = \hat{\mu}_b = \frac{K}{2} + H_c$ and $\hat{\sigma}_a = \hat{\sigma}_b = \frac{\left(\frac{K}{2} - H_c\right)}{2}$, where H_c is the measured coercivity of the magnet.

The results for the two magnetic samples are shown in Figs. 5-6. The homogeneous magnet hysteresis curve obtained with the "new" method is better than the "old" one especially at the lower (upper) part of the descending (ascending) curve (Fig. 5). This is due to the ability to establish an appropriate value for the standard deviations where the "old" method was very vague. The fit is worse in the upper (lower) part of the descending (ascending) curve. This is where most of the processes taking place are reversible. In

ferromagnets, the reversible processes are due to reversible bending of the domain walls and reversible rotation of the magnetization vectors of misaligned grains or particles. This effect is captured better by the vector model used in the "old" results. Fig. 6 shows a comparison between the "old" and "new" results against a measured major loop. Here the fit is definitely better with the "new" method.

Table 1 shows the parameter values obtained for each magnet.
The initial estimate of the mean, μ, is close to the final value obtained by the least-squares algorithm. This is not true for the σ-value. Notice also the differences in the K-values between the two magnets. In the homogeneous case, $K \approx 5 \cdot H_c$, while in the inhomogeneous case $K \approx 10 \cdot H_c$. This is because the loop squareness, S, of the second is smaller, *i.e.* a wider distribution with respect to the plane size is needed.

Table 1: Initial Estimates and Final values of the density parameters used in the identification of two different magnetic samples

	Homogeneous magnet (K=71, Hc=15)		Inhomogeneous magnet (K=31, Hc=3)	
	Initial	Final	Initial	Final
μ	50.5	49.859	18.5	19.651
σ	6.8	5.721	4.2	2.915

Simulation of hysteresis in SMAs

The experimental hysteresis loops in SMAs have significant differences from the ones discussed already. The input variable is temperature and the output variable is deformation (strain). The output is normalized to the maximum % strain observed and ranges from 0 to 1. The loop is skewed and shifted to the right of the output axis. SMA loops are traced in the opposite direction compared to magnetic loops. The ascending branch comes first and is the one to the right. A hysteresis operator appropriate for this type of behavior is the one in Fig. 2e. Since a < b, the Preisach plane has to be adjusted appropriately (Fig. 3b).

Because of the asymmetry in the loops the "old" identification procedure could not be applied here. Four distinct parameters, $\mu_a, \mu_b, \sigma_a, \sigma_b$, must be determined. Let T_a be the temperature at which the normalized % strain has reached 0.5 on the ascending branch and T_m the temperature at which the normalized % strain has reached 0.5 on the descending branch. Because $T_m > T_a$, $\mu_b > \mu_a$. Also, the loops are wider at the top which suggests that $\sigma_b > \sigma_a$. For the initial estimates the following rules were constructed along the lines of the rules used in the modeling of magnetic hysteresis:

$$\hat{\mu}_a = \frac{K}{2} - T_m \,,\ \hat{\mu}_b = \frac{K}{2} - T_a \,,\ \hat{\sigma}_a = \frac{\frac{K}{2} - T_m}{3} \,,\ \hat{\sigma}_a = \frac{\frac{K}{2} - T_a}{3} \,.$$

Table 2 summarizes the parameter optimization results for the SMA curves.

Table 2: Initial Estimates and Final values of the density parameters used in the identification of the SMA sample.

	K=81, T_a=0, T_m=20	
	Initial	Final
μ_a	20.5	20.401
σ_a	6.7	7.726
μ_b	40.5	40.339
σ_b	13.3	11.377

The "new" method reproduced the qualitative hysteresis behavior of the material in the major (Fig. 7) and minor loops (Fig. 8). The discrepancies are attributed to the choice of

hysteresis operator. The hysteresis process in SMAs should be able to be modeled by a scalar operator, so using a vector one doesn't solve the problem. Better results could be obtained when using the KP operator [10].

5 CONCLUDING REMARKS

Preisach-type models have been used to reproduce the hysteretical response in two different types of materials. The materials, magnetic and shape memory alloys, are not only very different in their microstructure but also present very different hysteresis characteristics. The models are based on the Preisach formalism but are adjusted to each material through the choice of an appropriate hysteresis operator. Then the model is identified for the specific materials with the help of a major loop measurement and a least-squares fitting procedure. The results demonstrate the ability of a modularly contructed abstract model to tune into a system through the choice of a hysteresis operator combined with a systematic identification method.

Work in progress involves the testing and development of more operators, scalar and vector, and the refinement of the identification procedure. Other bivariate densities as well as products of single-variable densities are also being tested.

Acknowledgements
The authors would like to thank Prof. Lagoudas of the Department of Aerospace Engineering, Texas A&M University, for kindly providing the experimental SMA hysteresis data used in this work.

References

1. F. Preisach, *Über die magnetische Nachwirkung*, Zeitschrift für Physik, 94 (1935), pp. 277-301.
2. Z. Bo, D. C. Lagoudas, Thermomechanical modeling of polycrystalline SMAs under cyclic loading, Part IV: modeling of minor hysteresis loops, Int. J. Eng. Sci. 37 (1999), pp. 1205-1249.
3. R.A. Guyer, K.R. McCall, B.N. Boitnott, Hysteresis, Discrete memory, and nonlinear Wave propagation in Rock: A New Paradigm, Phys. Rev. Let. 24(17) (1995), pp. 3491-3495.
4. Rod Cross, On the Foundations of Hysteresis in Economic Systems, Economics and Philosophy, Spring 1993, pp. 53-73.
5. Stanley H. Charap and Aphrodite Ktena, *Vector Preisach modeling*, Journal of Applied Physics, 73 (1993), pp. 5818-5823.
6. A. Ktena, D. I. Fotiadis and C. V. Massalas, A 2-D Model for Inhomogeneous Permanent Magnets, *Journal of Applied Physics*, 87(9) (2000), pp. 4780-4782.
7. A. Ktena, D. I. Fotiadis and C. V. Massalas, IEEE Trans. Mag., 36(6) (2000).
8. Aphrodite Ktena and Stanley H. Charap, Vector Preisach Modeling and Recording Applications, IEEE Trans. Magn., 29 (6) (1993), pp. 3661-3663.
9. DelVecchio, An Efficient Procedure for Modeling Complex Hysteresis Processes in Ferromagnetic Materials, IEEE Trans. Mag. 16(5) (1980), pp. 809-811.
10. G. V. Webb, D. C. Lagoudas and A. Kurdila, Hysteresis Modeling of SMA Actuators for Control Applications, J. Intelligent Material Systems and Structures, 9 (1998), pp. 432-448.
11. Y. O. Amor, M. Feliachi and H. Mohellebi, A new Convergence Procedure for the Finite Element Computing Associated to Preisach Hysteresis Model, IEEE Trans. Mag. 36(4) (2000), pp. 1242-1245.
12. D. H. Everett, A general approach to hysteresis, Trans. Faraday. Soc., 51 (1955), pp. 1551-1557.
13. Augusto Visintin, Differential Models of Hysteresis, Springer-Verlag, Berlin, 1994, pp. 10-29.
14. J.-G. Zhu and H.N. Bertram, Micromagnetic Studies of Thin Metallic Films, J. Appl. Phys. 63 (1988), pp. 3248-3253.
15. W. F. Brown, Micromagnetics, John Wiley &Sons, New York, 1963.
16. Augusto Visintin, *op. cit.*, pp. 59-82.
17. M. Krasnoselskii and A. Pokrovskii, Systems with Hysteresis, Nauka, Moscow, 1983.
18. I. D. Mayergoyz, *Mathematical models of hysteresis*, Physical Review Letters, 56(15) (1986), pp. 1518-1521.
19. E. C. Stoner and E. P. Wohlfarth, *A mechanism of magnetic hysteresis in heterogeneous alloys*, Phil. Trans. Roy. Soc., A240 (1948), pp. 599-642.
20. Augusto Visintin, op. cit., 119-122.
21. A. Bergqvist and G. Engdahl, A phenomenological differential-relation-based vector hysteresis model, J.Appl.Phys. 75(10), (1994), pp. 5484-5486.
22. E. Della Torre, R. A. Fry, O. Alejos and E. Cardelli, Identification of Parameters in Multilayer Media, IEEE Trans. Mag., 36(4) (2000), pp. 1272-1275.

23. E. H. Feutrill, P. G. McCormick and R. Street, Magnetization behavior in exchange-coupled $Sm_2Fe_{14}Ga_3C_2$/α-Fe, J.Phys.D: Appl. Phys. 29 (1996), pp. 2320-2326.

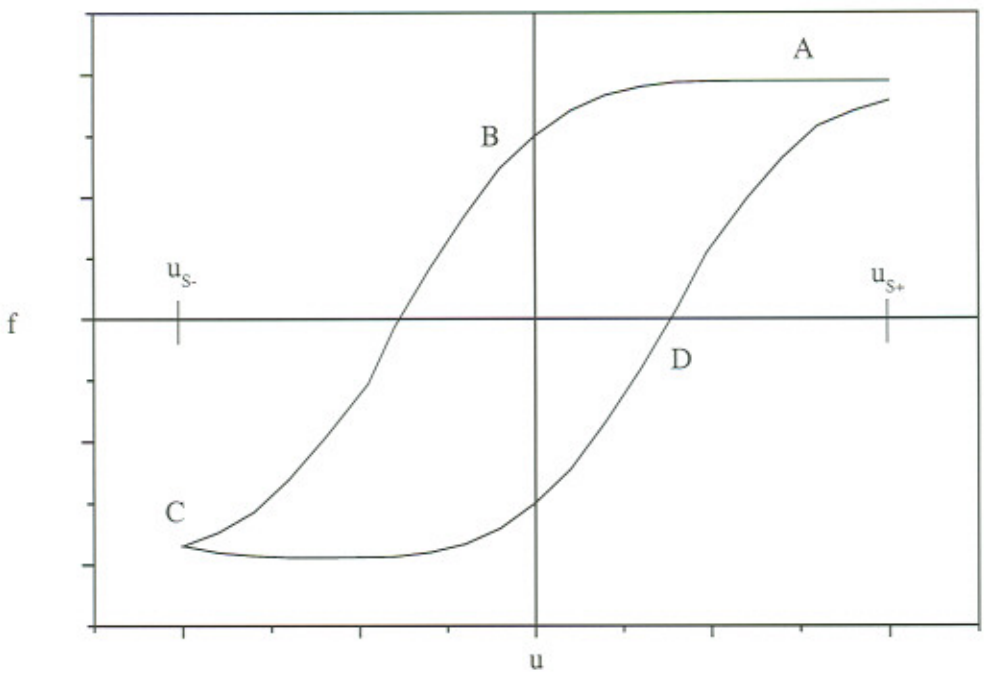

Figure 1: A typical hysteresis loop traced along the path ABCDA.

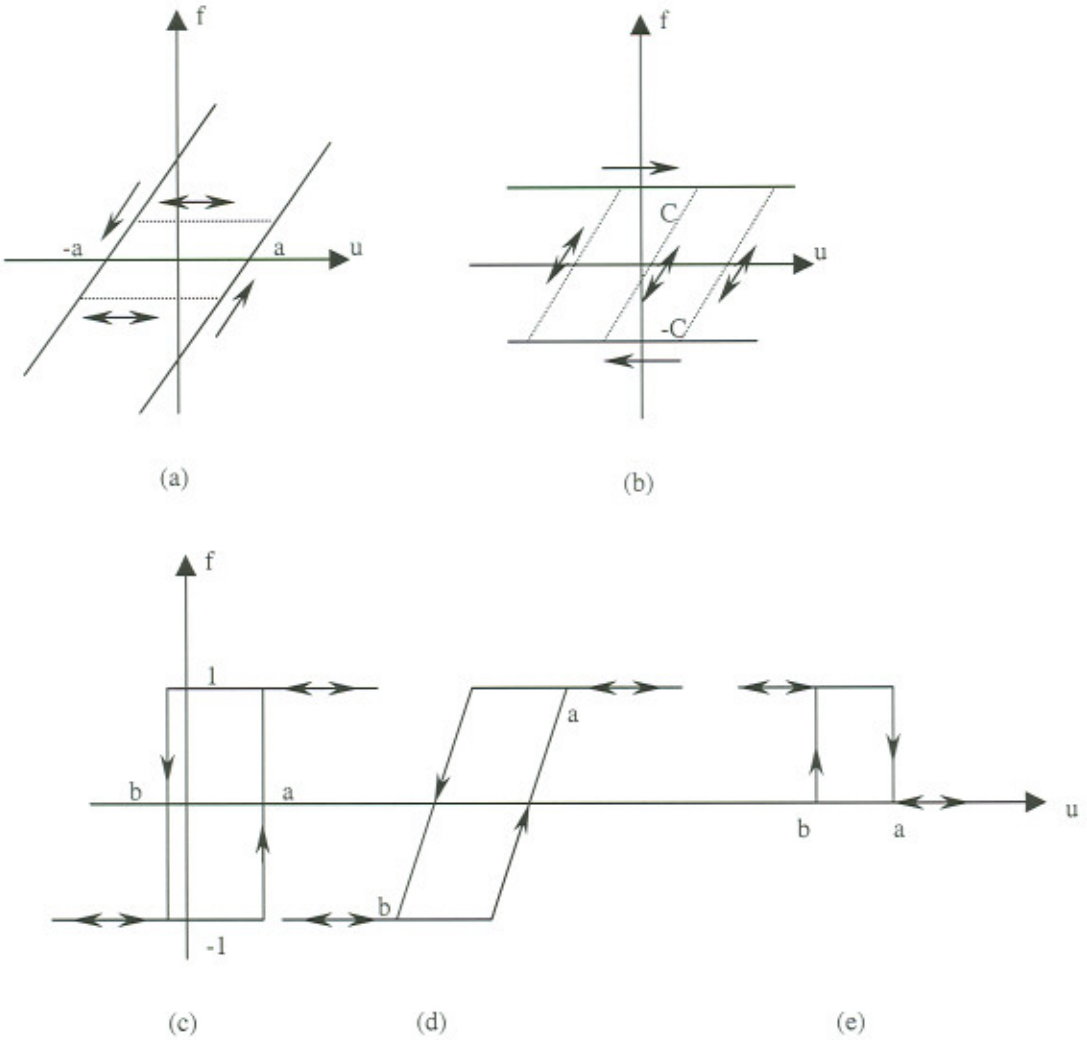

Figure 2: Hysteresis operators: (a) play, (b) stop, (c) Preisach, (d) KP and (e) modified Preisach.

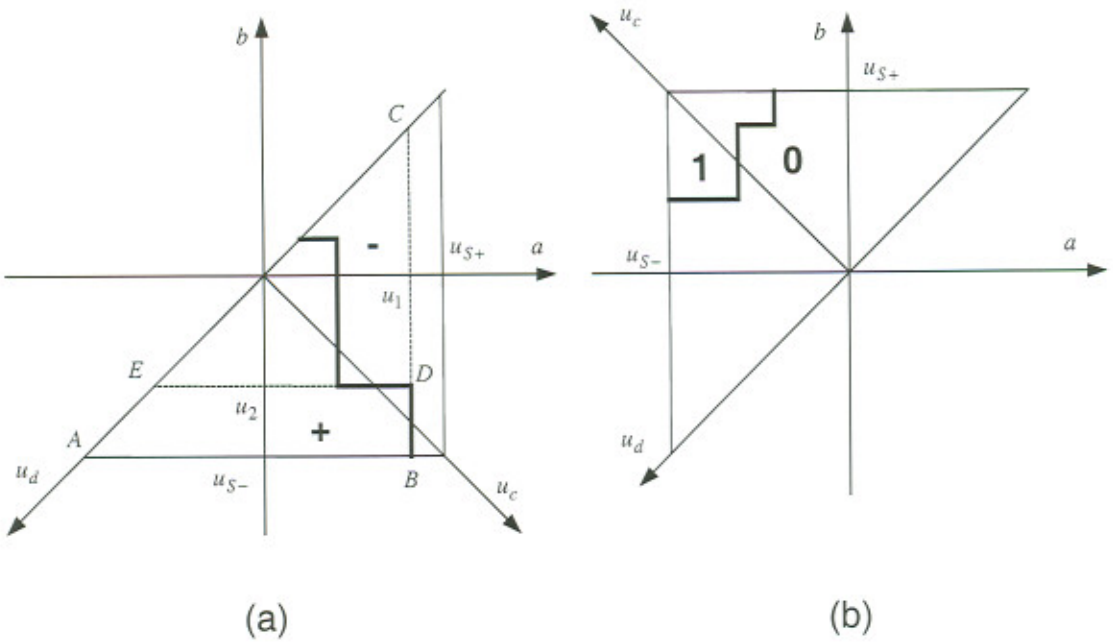

Figure 3: (a) The classical Preisach plane with the staircase bounday and (b) the Preisach plane used with the operator of Fig. 2e.

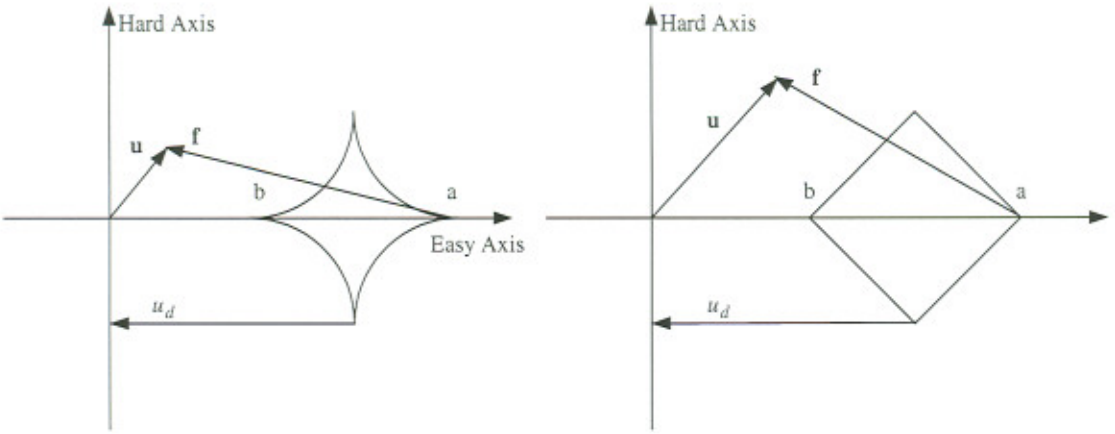

(a) (b)

Figure 4: Vector operators: (a) the S-W astroid and (b) the diamond.

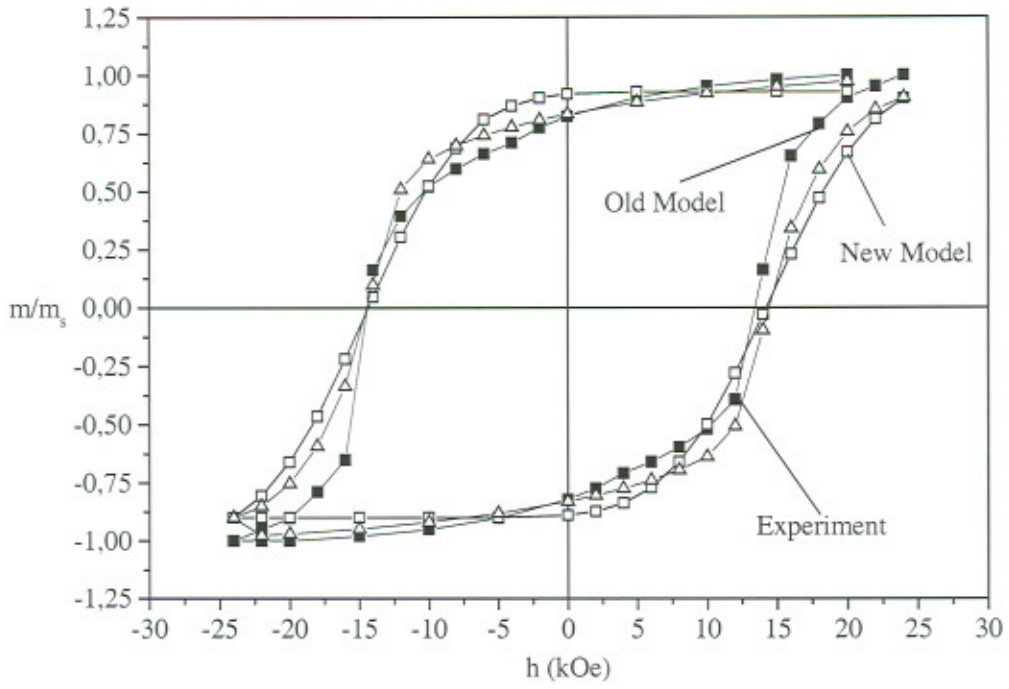

Figure 5: Homogeneous magnet. Experimental and simulated loops produced with the "old" and the "new" identification method.

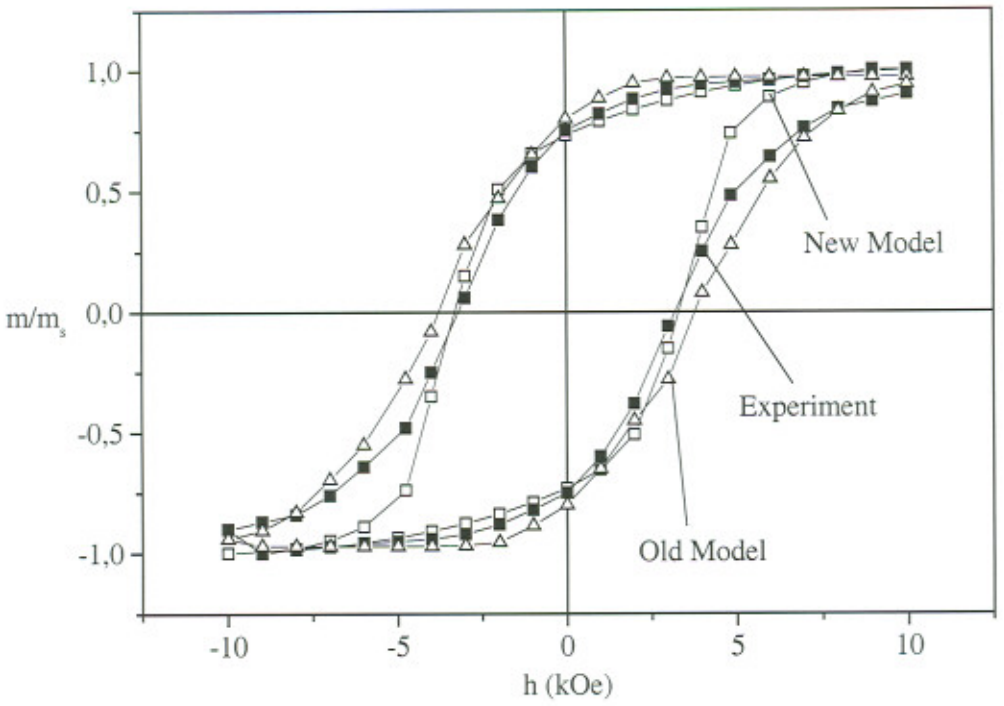

Figure 6: Inhomogeneous magnet. Experimental and simulated loops produced with the "old" and the "new" identification method.

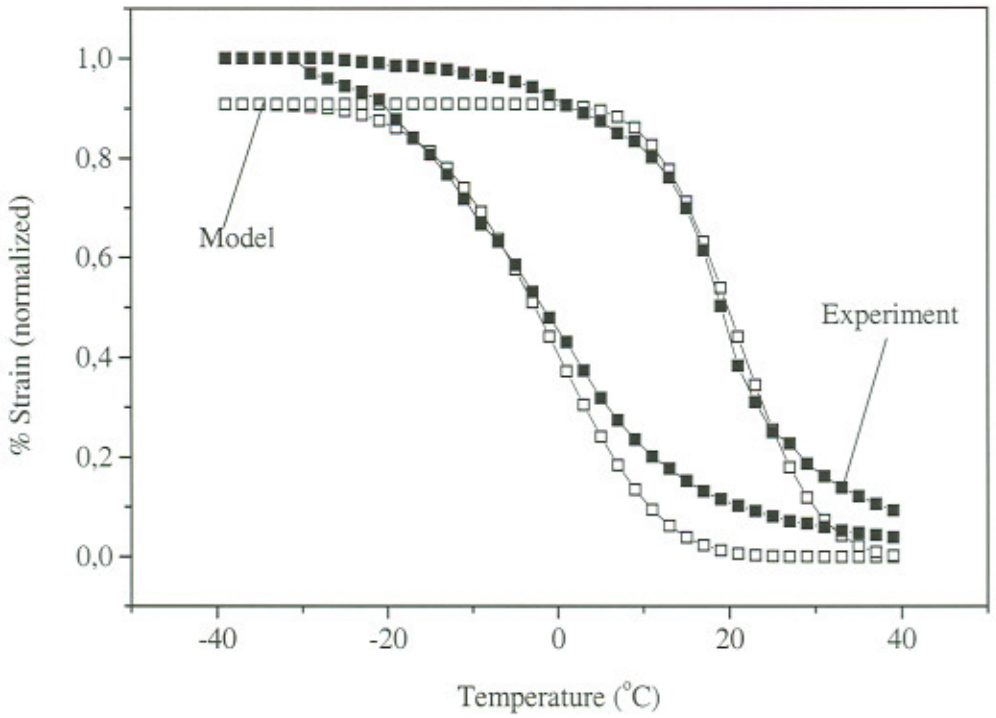

Figure 7: SMA. Experimental and simulated major loop.

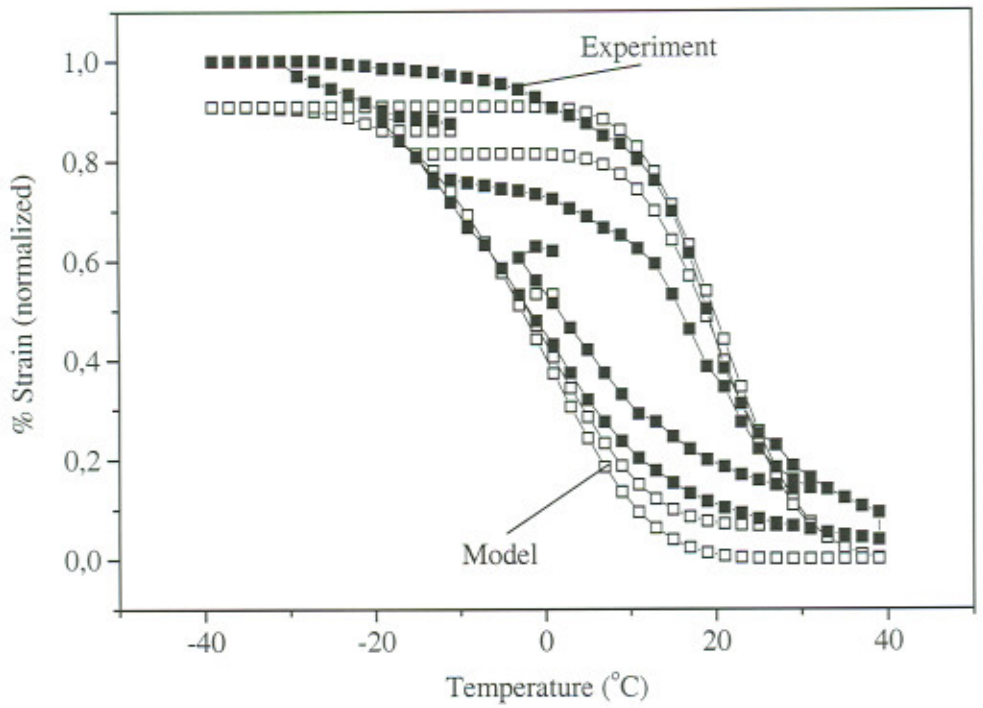

Figure 8: SMA. Experimental and simulated major and minor loops.